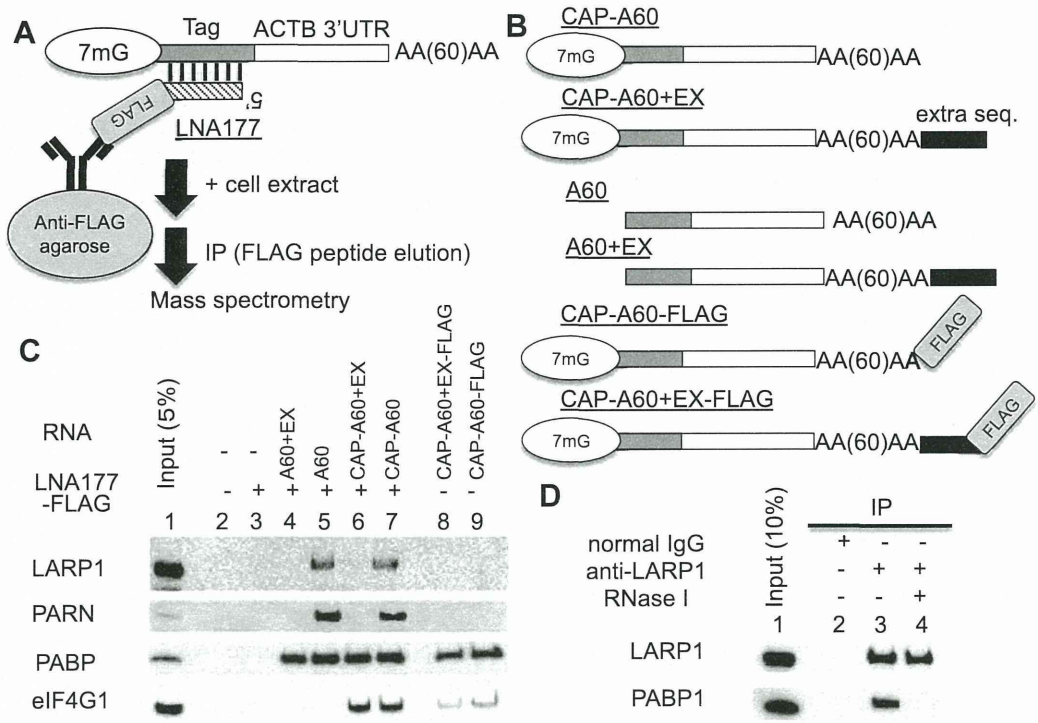

Fig. 1. Identification of proteins assembled on artificial poly(A)+ mRNA by LNA/RNA immunoprecipitation following ultra sensitive mass spectrometry. (A) Purification strategy for RNA immunoprecipitation using FLAG-tagged antisense LNA177. FLAG-tagged LNA177 and bait mRNA were annealed and then bound to anti-FLAG M2 agarose. The complex was then incubated with a HEK293 cell lysate. After washing, immunoprecipitated proteins were digested with lysyl endopeptidase and analyzed by LC–MS. (B) Schematic of the *in vitro* transcribed bait RNA used in the RNA immunoprecipitation assays. All chimeric mRNA shared the 3′ UTR of ACTB mRNA, a complementary sequence to LNA177, and a 60-nt poly(A) tail. The 35-nt of extra sequence (5′-GAGACCACUGUCAUGCCGUUACGUAGAAUCGAAUU) was derived from pGEM T-Easy vector (Promega) and primer 2199 using cDNA cloning for the ACTB 3′UTR possessing poly(A) tail. (C) Co-immunoprecipitated proteins with various bait RNAs were analyzed by Western blotting. Lane 1, input; 2, no bait; 3, LNA177; 4, LNA177 + A60 + EX RNA; 5, LNA177 + A60 RNA; 6, LNA177 + CAP-A60 + EX RNA; 7, LNA177 + CAP-A60 RNA; 8, LNA177 + CAP-A60 + EX-FLAG RNA and 9, LNA177 + CAP-A60-FLAG RNA. (D) RNA dependent interaction of LARP1 and PABP1. Immunoprecipitation of LARP1 was performed with an anti-LARP1 antibody (A302-088A, Bethyl Laboratories Inc.). IgG was used as a control. Part of the immunoprecipitated sample was treated with RNase I to digest the poly(A) sequences. The immunoprecipitated proteins were analyzed by Western blotting using antibodies against LARP1 and PABP1. Lane 1, input; 2, normal IgG; 3, anti-LARP1; and 4, anti-LARP1 + RNase I treatment.

Next, we confirmed the intracellular interaction of LARP1 with PABP1 by immunoprecipitation using an anti-LARP1 antibody. The LARP1–PABP1 interaction of was disintegrated by RNase I treatment, suggesting that the interaction was RNA dependent (Fig. 1D).

3.3. Sequence specificity of LARP1 RNA recognition

To assess the length of poly(A) tail required for LARP1 binding, we carried out further RNA immunoprecipitation with RNA possessing poly(A) tail of various lengths. It was apparent that LARP1 binding required a poly(A) tail longer than 9-nt (Fig. 2A and B). To determine the nucleotide selectivity of LARP1, we prepared various RNA baits with different nucleotide compositions and analyzed their interaction with LARP1 by RNA immunoprecipitation. LARP1 did not bind to mutant RNAs possessing poly(G), poly(C) or poly(U) sequences at their 3′ termini (Fig. 2C and D). Furthermore, the LARP1 with poly(A)+ RNA interaction was abolished by adding a single guanosine, cytidine or uridine residue to the 3′ terminus of the RNA (Fig. 2C and D).

3.4. LARP1 stabilizes multiple 5′TOP mRNAs

To confirm the specific interaction of LARP1 with poly(A)+ mRNA under physiological conditions, we immunoprecipitated endogenous LARP1 protein using two different LARP1 antibodies (Fig. 3A). Co-immunoprecipitated RNAs were purified and analyzed by qRT-PCR. We confirmed that all of the mRNAs possessing a 3′ poly(A) tail that were examined were enriched in the anti-LARP1 immunoprecipitations (Fig. 3B). In contrast, no enrichment of RNA species lacking poly(A) tail, such as ribosomal RNAs, nuclear non-coding RNAs (ncRNAs) and histone mRNAs, were detected.

We hypothesized that LARP1 was involved in stabilization of poly(A)+ mRNAs through binding to the 3′ terminus of the poly(A) tail. To confirm this, we conducted LARP1 depletion using RNAi in HEK293 cells (Fig. 4A and B). Then we investigated the accumulation levels of numerous transcripts, which were commonly used for reference (Fig. 4C, E and F).

Unexpectedly, PP1A, YWHAZ, PGK1, TBP1, GAPDH, HSP90AB1, TBX1 and PRCP mRNAs were slightly altered by depletion of LARP1, although these mRNAs were co-immunoprecipitated with the anti-LARP1 antibody (Figs. 3B and 4E). We also confirmed that the levels of several ncRNAs and histone mRNAs, which were not co-immunoprecipitated with anti-LARP1 antibody, were unaltered (Figs. 3B and 4F). Interestingly, the levels of mature mRNAs for RPS6, RPL7 and HNRNPA1 were substantially diminished, while the levels of the corresponding unspliced pre-mRNAs remained constant in the LARP1-depleted cells (Fig. 4C).

RPS6, RPL7 and HNRNPA1 mRNAs were categorized as 5′TOP mRNAs [18,19]. Therefore, we examined the expression levels of other eight 5′TOP RNAs, and found that the expression levels of those examined were commonly reduced by LARP1 depletion (Fig. 4D).

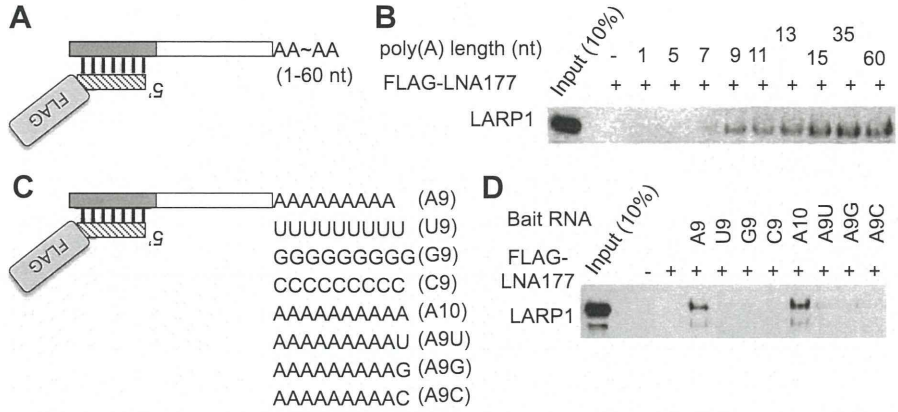

Fig. 2. LARP1 specifically recognized the 3′ terminus of a poly(A) tail. (A) Schematic of bait RNAs with poly(A) tails of various lengths. (B) The binding specificity of LARP1 to poly(A) tails of various lengths was examined by RNA immunoprecipitation and the products were analyzed by Western blotting using an antibody against LARP1. (C) Schematic of mutant mRNAs with a variety of 3′ termini. An A9 RNA with a 9-nt poly(A) tail was used as a positive standard. The 3′ terminus of three variants (U9, G9, and C9; upper panel) was consist of 9 nt for poly(G), poly(C) or poly(U), instead of poly(A). The four variants (10A, A9G, A9C and A9U; lower panel) contained an extra nucleotide at the 3′ end of the poly(A) tail. (D) RNA immunoprecipitation and Western blot analysis as shown in (B).

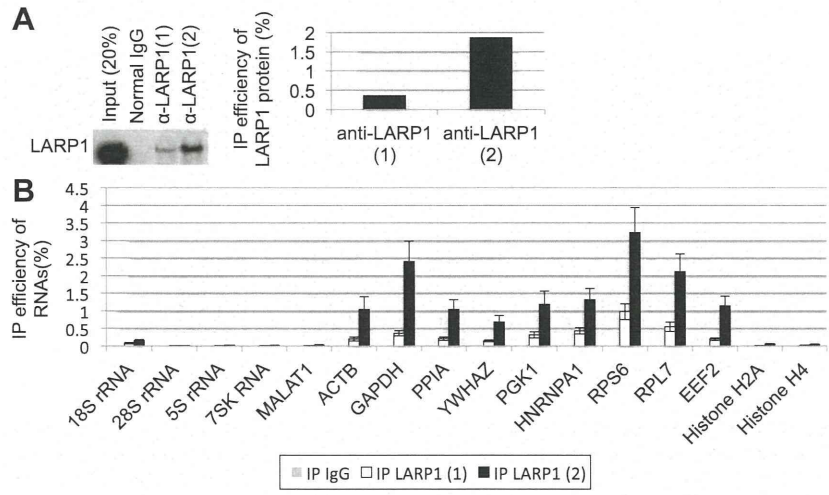

Fig. 3. LARP1 commonly interacts with poly(A)+ RNA. (A) Immunoprecipitation with normal IgG as a control and two different antibodies against LARP1 (1; A302-087A or 2; A302-088A, Bethyl Laboratories Inc.) were conducted. The representative immunoprecipitated LARP1 proteins were evaluated by Western blotting (left) and the immunoprecipitation efficiency of LARP1 was quantified by Multi Gauge ver. 3.0 software (Fujifilm, Japan. right). (B) RNAs that co-immunoprecipitated with LARP1 were purified for qRT-PCR analysis. Multiple sets of primers for ribosomal RNAs, nuclear ncRNAs, mRNAs encoding reference genes, and histone mRNAs, were prepared as shown in Supplementary Table 1. Bars represent means ± S.D. of three independent experiments.

4. Discussion

In this study, we attempted to identify the proteins that bind to the poly(A) termini of mRNA molecules by RNA-immunoprecipitation and following ultra-sensitive mass spectrometry. A comparison of proteins that interact with CAP-A60 RNA and CAP-A60 + EX RNA revealed several candidate proteins, which specifically interacted with the 3′ terminus of a poly(A) tail (Supplementary Table 2).

Among these candidate proteins, we observed that LARP1 specifically recognized the 3′ termini of poly(A) tails (Fig. 1C). We also showed that a length >9-nt in the 3′ terminal poly(A) tail was necessary for the LARP1 binding (Fig. 2B). Additionally, a slight increase in the LARP1 signal was observed when the poly(A) tail length was increased from 13-nt to 15-nt. However, further elongation of the tail did not affect LARP1 binding (Fig 2B). Hence, we consider that a poly(A) of at least 9-nt is the minimum for the RNA recognition by LARP1, while 15-nt poly(A) is sufficient.

Previous studies have shown that the conserved La motif of La protein specifically recognizes the 3′ terminal UUU sequence on the nascent transcripts of RNA polymerase III [5]. It is noteworthy that the 3′-hydroxyl group and a penultimate base mainly affected to the La protein affinity for RNA, while the last nucleotide appeared to be less important [8–10]. It should be noted that addition of an extra G, C or U at the 3′ terminus of the poly(A) tail diminished LARP1 recruitment onto the synthetic RNA (Fig. 2D), regardless of its possession of the highly conserved La motif [9]. Further analyses are required to clarify the mechanism by which the poly(A) terminal binds to LARP1.

We showed that the poly(A)+ mRNA interaction preference exhibited by LARP1 differed from those exhibited by PABP1 (Fig. 1C). These results imply that LARP1 is recruited onto the 3′ terminus of poly(A) tail, independently with of PABP1. However, a previous study reported that LARP1 directly interacted with PABP, as shown RNase A treatment, which cleaves specifically after pyrimidine nucleotides [15]. Because both LARP1 and PABP

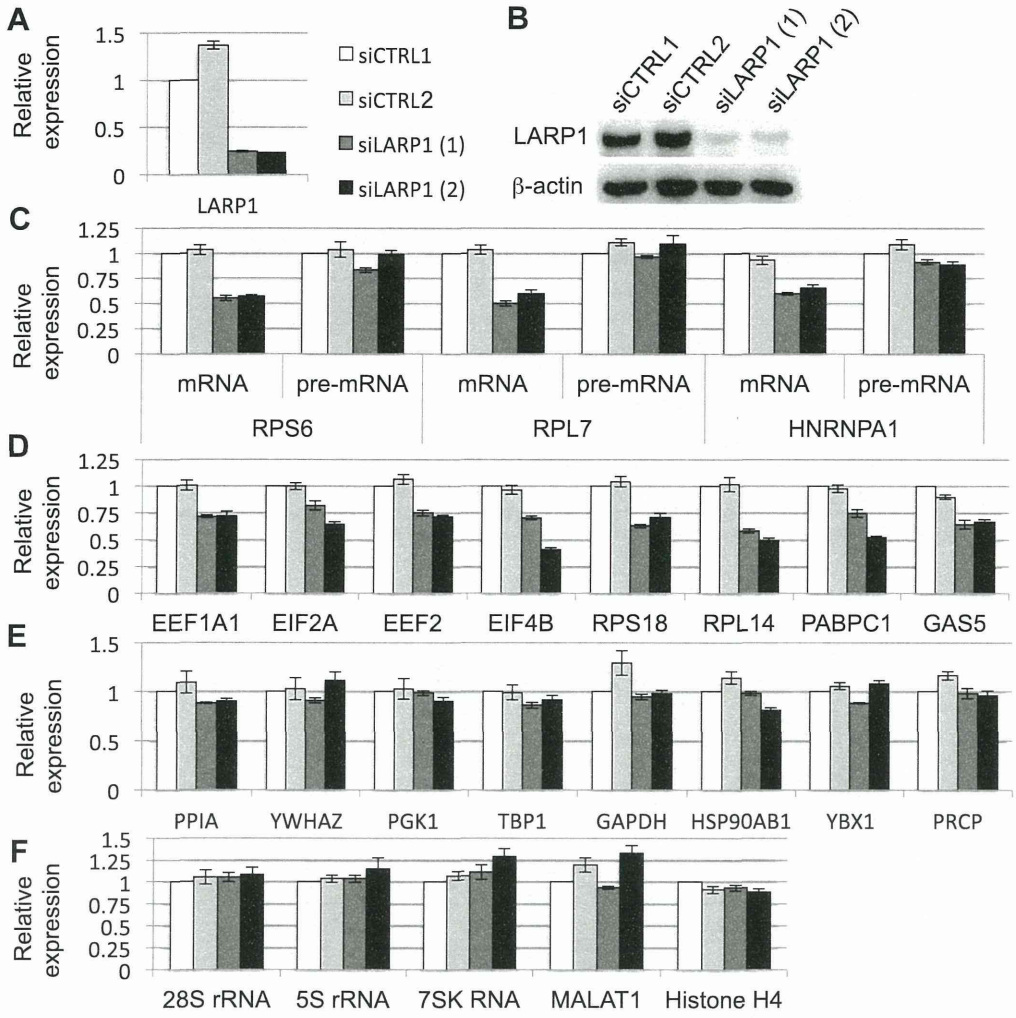

Fig. 4. LARP1 stabilized 5′TOP mRNAs. RNAi using negative control siRNAs (open and light gray bars) and two different siRNAs for LARP1 (dark gray and black bars) were conducted in HEK 293 cells. RNAi showing diminished levels of LARP1 mRNA (A) and protein (B). The expression levels of multiple RNAs were examined by qRT-PCR. Relative expression levels of the RNAs examined were normalized against 18S rRNA. Bars represent the means ± S.D. of three independent experiments. (C) Matured and immatured 5′ TOP mRNAs, (D) other 5′TOP RNAs, (E) reference mRNAs, and (F) non-coding RNAs and histone mRNA.

interacted with poly(A), our interaction analysis was performed by RNase I treatment, and revealed the RNA dependent interaction of LARP1 with PABP1 at least in human cells (Fig. 1D).

Meanwhile, in drosophila, it was reported that the interaction with dmLarp and pabp have been reported to resistant to RNase I digestion [13]. It is possible that a low conservation rate in the N-terminal region of LARP1 was the cause of the distinct affinity to PABP observed in our study.

The poly(A) tail plays a critical role in translational activation and stabilization of mRNA [1], whereas a previous study showed that LARP1 promotes the translation [14]. Our results showed that a large portion of mRNAs possessing poly(A) tail were co-immunoprecipitated with LARP1 (Fig. 3) and LARP1 depletion caused a decrease in the expression levels of 5′TOP mRNA (Fig. 4C and D). We asked whether the reduction of these mRNAs was regulated transcriptionally or post-transcriptionally. Accordingly, expression of RPS6, RPL7, and HNRNPA1 pre-mRNA was constant, thus that the reduction in mRNA was post-transcriptional event, and one of which was perhaps related to RNA stability.

We assumed that LARP1 might contribute to the mRNA stabilization by preventing the 3′–5′ exoribonuclease activity. To investigate whether the reduction of 5′TOP mRNA was due to shortening of the poly(A) tail, we conducted northern blot analysis of RPS6 and RPL7 mRNAs. However, no obvious shortening of these mRNAs was detected in the LARP1-depleted cells (data not shown).

It remains unclear as to why LARP1 depletion only affects 5′TOP mRNA, although LARP1 commonly interacted with poly(A)+ mRNA (Fig. 3B). The 5′TOP mRNAs tend to be the most abundant poly(A)-containing mRNAs in the cell. To examine the effects of RNA abundance, we examined GAPDH, HSP90AB1, YBX1 and PRCP mRNAs, which showed similar abundances to 5′TOP mRNAs in HEK293 cells; slight alternation of these mRNAs was revealed by RNAi for LARP1 (Fig. 4E).

A previous study showed that the LARP1 orthologous in *Caenorhabditis elegans* localizes to the P-body [20], where translationally inactivated mRNAs accumulate and are usually subjected to degradation [21,22]. It is consistent that LARP1 affects the stability of the translationally inactivated mRNA including majority of 5′TOP RNAs.

Previous reports have indicated that La protein has affinity for the 5′ cap and 5′ triphosphate of RNA molecules, and LARP7 interacted with 5′ end of RNA with methylphosphate capping enzyme dependent manner [23–25]. It is also reasonable to speculate that LARP1 may control mRNA stability by mediating the interaction

between 5′TOP at the 5′ terminus and poly(A) tail at the 3′ terminus of an mRNA.

In this study, we showed that the LARP1 recognized the 3′ terminus of an mRNA poly(A) tail and selectively stabilized 5′TOP mRNAs. The biological function and true significances of the LARP1–mRNA interaction at the 3′ terminus of the a poly(A) tail remains unclear. Investigation in the mechanisms involved in LARP1-mediated stabilization of 5′TOP mRNA and into the physiological role(s) of LARP1 are planned.

Acknowledgements

We thank the members of the Natsume laboratory for their valuable discussion and assistance. We also thank Dr. Tetsuro Hirose for providing useful advices and comments on the manuscript. This research was supported by a Grant from the New Energy and Industrial Technology Development Organization (NEDO).

Appendix A. Supplementary data

Supplementary data associated with this article can be found, in the online version, at http://dx.doi.org/10.1016/j.febslet.2013.05.035.

References

[1] Parker, R. and Song, H. (2004) The enzymes and control of eukaryotic mRNA turnover. Nat. Struct. Mol. Biol. 11, 121–127. Review.
[2] Jackson, R.J., Hellen, C.U. and Pestova, T.V. (2010) The mechanism of eukaryotic translation initiation and principles of its regulation. Nat. Rev. Mol. Cell Biol. 11, 113–127. Review.
[3] Mangus, D.A., Evans, M.C. and Jacobson, A. (2003) Poly(A)-binding proteins: multifunctional scaffolds for the post-transcriptional control of gene expression. Genome Biol. 4, 223. Review.
[4] Dominski, Z. and Marzluff, W.F. (2007) Formation of the 3′ end of histone mRNA: getting closer to the end. Gene 396, 373–390.
[5] Stefano, J.E. (1984) Purified lupus antigen La recognizes an oligouridylate stretch common to the 3′ termini of RNA polymerase III transcripts. Cell 36, 145–154.
[6] Krueger, B.J., Jeronimo, C., Roy, B.B., Bouchard, A., Barrandon, C., Byers, S.A., Searcey, C.E., Cooper, J.J., Bensaude, O., Cohen, E.A., Coulombe, B. and Price, D.H. (2008) LARP7 is a stable component of the 7SK snRNP while P-TEFb, HEXIM1 and hnRNP A1 are reversibly associated. Nucleic Acids Res. 36, 2219–2229.
[7] Bousquet-Antonelli, C. and Deragon, J.M. (2009) A comprehensive analysis of the La-motif protein superfamily. RNA 15, 750–764.
[8] Teplova, M., Yuan, Y.R., Phan, A.T., Malinina, L., Teplov, A. and Patel, D.J. (2006) Structural basis for recognition and sequestration of UUU(OH) 3′ temini of nascent RNA polymerase III transcripts by La, a rheumatic disease autoantigen. Mol. Cell 21, 75–85.
[9] Dong, G., Chakshusmathi, G., Wolin, S.L. and Reinisch, K.M. (2004) Structure of the La motif: a winged helix domain mediates RNA binding via a conserved aromatic patch. EMBO J. 23, 1000–1007.
[10] Bayfield, M.A., Yang, R. and Maraia, R.J. (2010) Conserved and divergent features of the structure and function of La and La-related proteins (LARPs). Biochim. Biophys. Acta 1799, 365–378.
[11] Ichihara, K., Shimizu, H., Taguchi, O., Yamaguchi, M. and Inoue, Y.H. (2007) A Drosophila orthologue of larp protein family is required for multiple processes in male meiosis. Cell Struct. Funct. 32, 89–100.
[12] Chauvet, S., Maurel-Zaffran, C., Miassod, R., Jullien, N., Pradel, J. and Aragnol, D. (2000) Dlarp, a new candidate Hox target in Drosophila whose orthologue in mouse is expressed at sites of epithelium/mesenchymal interactions. Dev. Dyn. 218, 401–413.
[13] Blagden, S.P., Gatt, M.K., Archambault, V., Lada, K., Ichihara, K., Lilley, K.S., Inoue, Y.H. and Glover, D.M. (2009) Drosophila Larp associates with poly(A)-binding protein and is required for male fertility and syncytial embryo development. Dev. Biol. 334, 186–197.
[14] Burrows, C., Abd Latip, N., Lam, S.J., Carpenter, L., Sawicka, K., Tzolovsky, G., Gabra, H., Bushell, M., Glover, D.M., Willis, A.E. and Blagden, S.P. (2010) The RNA binding protein Larp1 regulates cell division, apoptosis and cell migration. Nucleic Acids Res. 38, 5542–5553.
[15] Ideue, T., Adachi, S., Naganuma, T., Tanigawa, A., Natsume, T. and Hirose, T. (2012) U7 small nuclear ribonucleoprotein represses histone gene transcription in cell cycle-arrested cells. Proc. Natl. Acad. Sci. USA 109, 5693–5698.
[16] Kourouklis, D., Murakami, H. and Suga, H. (2005) Programmable ribozymes for mischarging tRNA with non-natural amino acids and their applications to translation. Methods 36, 239–244.
[17] Natsume, T., Yamauchi, Y., Nakayama, H., Shinkawa, T., Yanagida, M., Takahashi, N. and Isobe, T. (2002) A direct nanoflow liquid chromatography–tandem mass spectrometry system for interaction proteomics. Anal. Chem. 74, 4725–4733.
[18] Meyuhas, O. (2000) Synthesis of the translational apparatus is regulated at the translational level. Eur. J. Biochem. 267, 6321–6330. Review.
[19] Thoreen, C.C., Chantranupong, L., Keys, H.R., Wang, T., Gray, N.S. and Sabatini, D.M. (2012) A unifying model for mTORC1-mediated regulation of mRNA translation. Nature 485, 109–113.
[20] Nykamp, K., Lee, M.H. and Kimble, J. (2008) *C. elegans* La-related protein, LARP-1, localizes to germline P bodies and attenuates Ras-MAPK signaling during oogenesis. RNA 14, 1378–1389.
[21] Parker, R. and Sheth, U. (2007) P bodies and the control of mRNA translation and degradation. Mol. Cell 25, 635–646.
[22] Moser, J.J. and Fritzler, M.J. (2010) Cytoplasmic ribonucleoprotein (RNP) bodies and their relationship to GW/P bodies. Int. J. Biochem. Cell Biol. 42, 828–843.
[23] Fan, F., Goodier, J.L., Chamberlain, J.R., Engelke, D.R. and Maraia, R.J. (1998) 5′ Processing of tRNA precursors can be modulated by the human La antigen phosphoprotein. Mol. Cell. Biol. 18, 3201–3211.
[24] Bhattachary, R., Perumal, K., Sinha, K., Maraia, R. and Reddy, R. (2002) Methylphosphate cap structure in small RNAs reduces the affinity of RNAs to La protein. Gene Expr. 10, 243–253.
[25] Muniz, L., Egloff, S. and Kiss, T. (2013) RNA elements directing in vivo assembly of the 7SK/MePCE/Larp7 transcriptional regulatory snRNP. Nucleic Acids Res. 41, 4686–4698.

jmb Article

PLEIAD/SIMC1/C5orf25, a Novel Autolysis Regulator for a Skeletal-Muscle-Specific Calpain, CAPN3, Scaffolds a CAPN3 Substrate, CTBP1

Yasuko Ono[1,2], Shun-ichiro Iemura[1,3], Stefanie M. Novak[2], Naoko Doi[1], Fujiko Kitamura[1], Tohru Natsume[3], Carol C. Gregorio[2] and Hiroyuki Sorimachi[1]

*1 - **Calpain Project,** Department of Advanced Science for Biomolecules, Tokyo Metropolitan Institute of Medical Science (IGAKUKEN), 2-1-6 Kamikitazawa, Setagaya-ku, Tokyo 156-8506, Japan*
*2 - **Cellular and Molecular Medicine,** University of Arizona, Tucson, AZ 85724, USA*
*3 - **Biological Information Research Center,** National Institute of Advanced Industrial Science and Technology, 2-42 Aomi, Kohtoh-ku, Tokyo 135-0064, Japan*

***Correspondence to Yasuko Ono:** Calpain Project, Department of Advanced Science for Biomolecules, Tokyo Metropolitan Institute of Medical Science, 2-1-6 Kamikitazawa, Setagaya-ku, Tokyo 156-8506, Japan. ono-ys@igakuken.or.jp*
http://dx.doi.org/10.1016/j.jmb.2013.05.009
Edited by R. Huber

Abstract

CAPN3/p94/calpain-3 is a skeletal-muscle-specific member of the calpain protease family. Multiple muscle cell functions have been reported for CAPN3, and mutations in this protease cause limb-girdle muscular dystrophy type 2A. Little is known about the molecular mechanisms that allow CAPN3 to be so multifunctional. One hypothesis is that the very rapid and exhaustive autolytic activity of CAPN3 needs to be suppressed by dynamic molecular interactions for specific periods of time. The previously identified interaction between CAPN3 and connectin/titin, a giant molecule in muscle sarcomeres, supports this assumption; however, the regulatory mechanisms of non-sarcomere-associated CAPN3 are unknown. Here, we report that a novel CAPN3-binding protein, PLEIAD [*Pl*atform *e*lement for *i*nhibition of *a*utolytic *d*egradation; originally called SIMC1/C5orf25 (*S*UMO-*i*nteracting *m*otif *c*ontaining protein *1*/*c*hromosome *5* *o*pen *r*eading *f*rame *25*)], suppresses the protease activity of CAPN3. Database analyses showed that PLEIAD homologs, like CAPN3 homologs, are evolutionarily conserved in vertebrates. Furthermore, we found that PLEIAD also interacts with CTBP1 (*C-t*erminal *b*inding *p*rotein *1*), a transcriptional co-regulator, and CTBP1 is proteolyzed in COS7 cells expressing CAPN3. The identified cleavage sites in CTBP1 suggested that it undergoes functional modification upon its proteolysis by CAPN3, as well as by conventional calpains. These results indicate that PLEIAD can shift its major function from CAPN3 suppression to CAPN3-substrate recruitment, depending on the cellular context. Taken together, our data suggest that PLEIAD is a novel regulatory scaffold for CAPN3, as reflected in its name.

Introduction

CAPN3 (also called p94 or calpain-3) is an skm (*sk*eletal *m*uscle)-specific cysteine protease belonging to the calpain super family (EC 3.4.22.18, clan CA, family C2).[1] The calpains are intracellular Ca^{2+}-requiring cysteine proteases. Many studies have shown that proteolysis by calpain has a modulatory effect on the functions of the substrate proteins.[2–6] Therefore, calpain is considered to be a modulator protease rather than a degrading protease such as proteasomal and lysosomal proteases.[7]

From a physiological perspective, genetic defects in CAPN3 cause limb-girdle muscular dystrophy type 2A[8]; therefore, the importance of CAPN3's functions are well recognized.[9] To examine the consequences of altering the modulating functions of CAPN3 in skm, we have generated several different mouse limb-girdle muscular dystrophy type 2A models, including knockout mice ($Capn3^{-/-}$), which lack the full-length CAPN3 protein[10–17]; knockin mice ($Capn3^{CS/CS}$) in

which CAPN3 is replaced by a protease-inactive mutant CAPN3:C129S (CAPN3:CS)[18,19]; and transgenic mice in which CAPN3:CS is overexpressed.[20] Analyses of these models have shown that CAPN3 has different cellular functions depending on the subcellular compartment in which it is located. In particular, a surprising finding was that CAPN3 localizes to triads, where it plays an important role as a structural component and not as a protease.[19]

The two defined roles of CAPN3, that is, as a protease and as a structural protein, are not necessarily mutually exclusive. However, too little is currently known about the molecular properties of CAPN3 to explain the relationships among these two roles and another property of CAPN3—its very rapid autolysis.[21] In skm cells, CAPN3's stability as a pre-autolytic full-length molecule has been attributed to its interaction with connectin/titin, a giant sarcomeric protein,[22,23] since connectin/titin's ability to suppress the autolytic loss of CAPN3 has been shown biochemically.[24] Furthermore, the N2A region of connectin/titin has been suggested to function as a scaffold for CAPN3.[25,26] However, in skm cells, CAPN3 is stable not only in sarcomeres but also in the cytosol.[27] Therefore, it is predicted that there are other regulatory mechanisms working in parallel or in combination with the connectin/titin-based machinery, to support CAPN3's multiple functions, especially those occurring outside of sarcomeres.

We sought to identify CAPN3-interacting proteins using a highly sensitive and efficient method based on mass spectrometry for analyzing protein–protein interactions.[28] Among these proteins, PLEIAD (*Pl*atform *e*lement for *i*nhibition of *a*utolytic *d*egradation), which was the previously uncharacterized SIMC1/C5orf25 (*S*UMO-*i*nteracting *m*otif *c*ontaining protein *1*/*c*hromosome *5* *o*pen *r*eading *f*rame *25*),[29] demonstrated a suppressive effect on CAPN3's protease activity. We identified vertebrate orthologs of PLEIAD according to their similarity with the human C-terminal sequence, which harbors the CAPN3 inhibitory or regulatory activity. We also found that PLEIAD binds to CTBP1 (*C-t*erminal *b*inding *p*rotein *1*),[30,31] which is a good substrate for calpains, including CAPN3. These results suggest that SIMC1/C5orf25 is a suppressor for CAPN3 but, at the same time, scaffolds CAPN3 to direct and regulate its substrate-proteolyzing activity. Such properties, like those of the connectin/titin N2A region, would qualify PLEIAD as an important regulatory protein for CAPN3.

Results

Protease activity of CAPN3 is suppressed by a novel protein, PLEIAD

To explore molecular interactions relevant to CAPN3's function and regulation, we expressed FLAG-CAPN3:N358D (CAPN3:ND), an activity-attenuated mutant[32] (Fig. 1a), in HEK293 cells and analyzed anti-FLAG coimmunoprecipitates of HEK293 lysates by liquid chromatography coupled with tandem mass spectrometry.[28] Since the initial goal was to identify activation-dependent interactions, the cells were treated with the Ca^{2+}-ionophore A23187, and the results were compared to those obtained in cells without A23187 treatment. This approach identified a novel CAPN3-binding protein C5orf25, which we named PLEIAD (see below) (Fig. 1b). To confirm the interaction, we expressed both proteins in COS7 cells; the interaction between MYC-PLEIAD and FLAG-CAPN3, as well as the interaction between FLAG-PLEIAD and CAPN3,

Fig. 1. A novel human protein, PLEIAD/C5orf25, interacts with and suppresses CAPN3. (a) Structure of CAPN3 is schematically shown. Autolytic activity is based on the result when each construct is expressed in COS7 cells. Vertical arrows indicate predominant autolytic sites. PC1 and PC2, protease core domains 1 and 2; C2L, C2-domain-like; PEF (L), penta-EF-hand; NS/IS1/IS2, CAPN3-specific insertion sequences; C129/H334/N358, active-site amino acid residues Cys, His, and Asn; CAPN3:CS, protease-inactive mutant; CAPN3:ND, a mutant with attenuated protease activity. (b) Domain structure of hPLEIAD and its genomic structure. Transcript variants are also depicted. The sequence information is summarized in Table 2. hPLEIADa to e, known splicing variants. hPLEIADf, the novel splicing variant of PLEIAD identified in this study, which lacks exons 2 and 3. "S1" to "S3" and "AS1" to "AS4" represent the positions of sense and antisense primers, respectively, used in the study. The sequences are summarized in Table 1. Ser and Pro, Ser-rich and Pro-rich region, respectively; PEST, a region rich in Pro, Glu, Ser, and Thr; NLS, putative nuclear localization signal sequence. Two phosphorylation sites are identified in hPLEIAD, S651 and S791. (c) hPLEIADf was coexpressed with CAPN3:WT(WT) or CAPN3:CS(CS) in COS7 cells and immunoprecipitated by anti-FLAG (FLAG-IP). Both CAPN3:WT and CAPN3:CS were coimmunoprecipitated with hPLEIADf. Note that the full-length 94-kDa band was hardly detectable when CAPN3:WT was expressed alone (lane 1, anti-pIS2). In the presence of coexpressed hPLEIADf, the 94-kDa band became visible and appeared to be coimmunoprecipitated more efficiently than the 55-kDa autolyzed fragment (lanes 4 and 9). (d) When coexpressed with PLEIADa or hPLEIADf in COS7 cells, the intensity of the full-length 94-kDa band of CAPN3:WT relative to that of the 55-kDa autolyzed fragment increased (lanes 4 and 5, anti-CAPN3). In the same samples, generation of the proteolyzed fragment of fodrin was suppressed (lanes 4 and 5, anti-proteolyzed fodrin). When the amount of the expression plasmid for hPLEIADf was reduced, the effects were smaller, and a decrease in expressed hPLEIADf was observed (lane 6). Closed and open arrowheads indicate the full-length and autolytic fragments of CAPN3, respectively, detected by Western blotting using an anti-pIS2 antibody. (e) Signal intensity of the full-length 94-kDa band evaluated using the intensity of the autolytic 55-kDa band in the same lane as a standard (e).

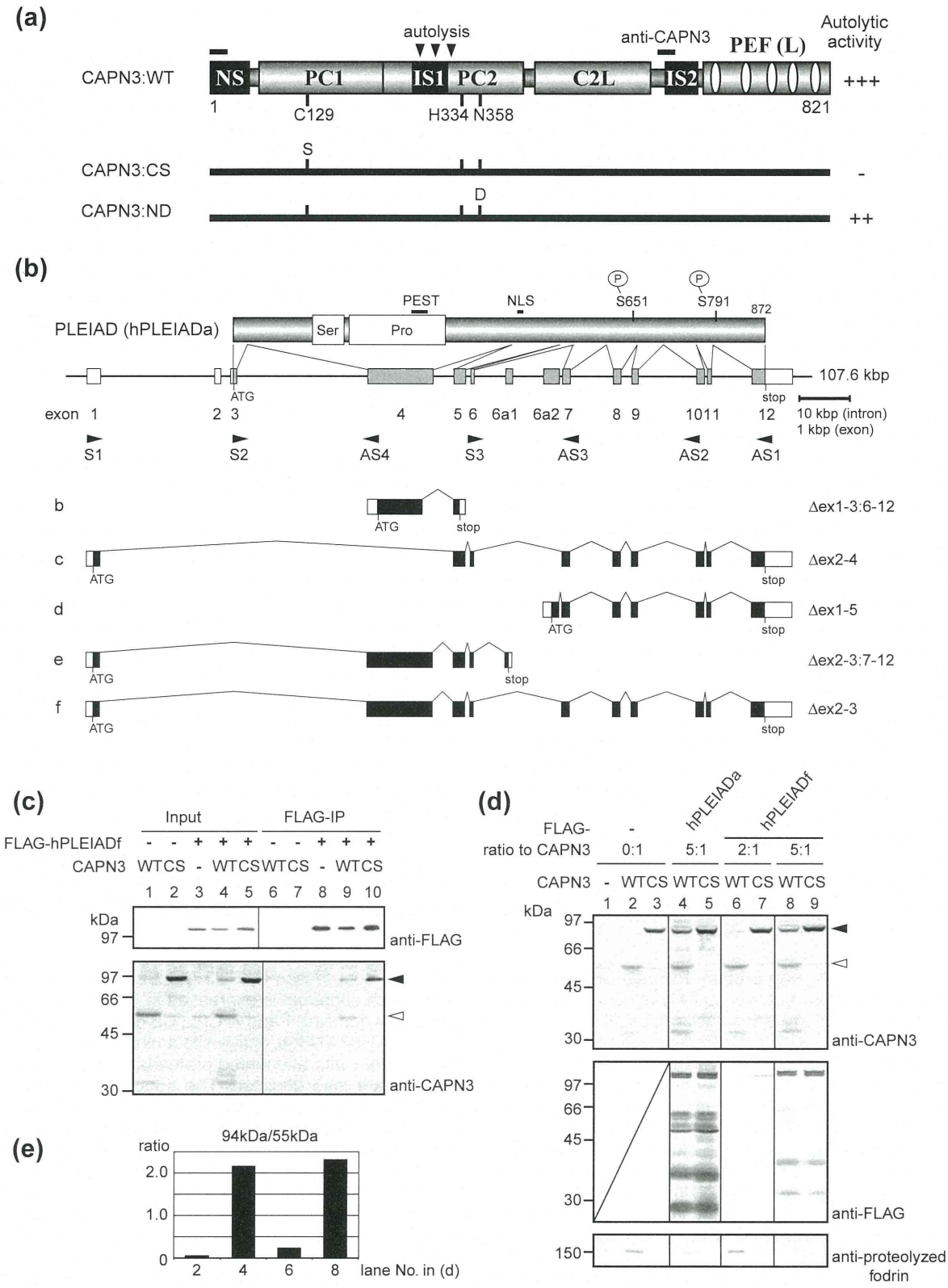

Fig. 1 (*legend on previous page*)

was reproducible without A23187 treatment (data not shown). Therefore, A23187 was omitted in the subsequent experiments.

The human PLEIAD gene (*PLEIAD*) is composed of 12 exons, of which exon 3 encodes the canonical first Met (Fig. 1b). In the National Center for Biotechnology Information (NCBI) and UniProtKB databases, the sequences for several alternative transcripts and corresponding proteins are deposited.[33] None of them, however, contains the sequence corresponding to exons 2 and 3. By PCR using a human skm cDNA library, we identified a novel variant lacking exons 2 and 3, but none of the other variants was found in the database [Fig. 1b, (5)]. This isoform will be temporarily designated as hPLEIADf.

Anti-FLAG coimmunoprecipitation experiments demonstrated the interaction of FLAG-hPLEIADf with CAPN3:WT and CAPN3:CS (Fig. 1c, lanes 9 and 10, anti-CAPN3). Therefore, the interaction between PLEIAD and CAPN3, which was originally detected in HEK293 cells, is predicted to take place in skm cells. Notably, the amount of FLAG-hPLEIADf was decreased when coexpressed with CAPN3:WT (compare lanes 4 and 5, anti-FLAG), and the relative intensity of the full-length 94-kDa band of CAPN3:WT was increased in the same sample (compare lanes 1 and 4, anti-CAPN3). This phenomenon is likely to indicate that CAPN3 activity reduces the amount of PLEIAD, either directly by proteolyzing it or indirectly by reducing the efficiency of PLEIAD's expression, and that PLEIAD reduces the autolytic activity of CAPN3.

These trends were confirmed by several independent transfections, and one representative result is shown in Fig. 1d. The signal intensity of the full-length 94-kDa band was evaluated using the intensity of the autolytic 55-kDa band in the same lane as a standard (Fig. 1e). Both hPLEIADa and hPLEIADf increased the amount of the 94-kDa CAPN3:WT, which was dependent on the level of hPLEIADf (lanes 4, 6, and 8, anti-CAPN3). Since the CAPN3-dependent proteolysis of fodrin was also suppressed (lanes 4 and 8 compared with lane 2, anti-proteolyzed fodrin), it was concluded that the protease activity of CAPN3 is suppressed by PLEIAD. Multiple bands were observed for hPLEIADa and hPLEIADf (Fig. 1d, lanes 4, 5, 8, and 9), independent of CAPN3's protease activity. Since FLAG tags were introduced to the N-termini of the hPLEIADs, the observed molecular sizes of these bands suggested that the region encoded by exon 4 is susceptible to nonspecific proteolysis in the cell.

The C-terminal region of PLEIAD regulates CAPN3's autolysis

To define the functional domains of PLEIAD with respect to their effect on CAPN3 autolysis, we coexpressed two different PLEIAD regions with CAPN3 in COS7 cells.

When the C-terminal region, designated as hPLEIAD-C, was coexpressed with CAPN3, the amount of CAPN3 detected by anti-CAPN3 increased. That is, the relative intensity of the 94-kDa band of CAPN3:WT increased, indicating reduced autolytic activity, but not as much as with the coexpression of hPLEIADa or hPLEIADf (Fig. 2b, lane 3 *versus* Fig. 1d, lanes 4 and 8, anti-CAPN3). In contrast, the N-terminal region of hPLEIAD, called hPLEIAD-N, had no effect on the expression pattern or intensity of CAPN3 (lane 4). These findings suggested that the conserved C-terminal sequence retained the CAPN3-suppressing activity, although it was weaker than the suppression exerted by full-length hPLEIADa and hPLEIADf.

For the mouse PLEIAD ortholog (mPLEIAD, originally called LOC319719), the structure of its gene, *Pleiad* (originally called *4732471D19Rik*), is similar to that of human *PLEIAD* (Fig. 2c). There are,

Fig. 2. The C-terminal region of PLEIAD is responsible for regulating CAPN3's autolytic activity. (a) Two regions of PLEIAD, hPLEIAD-N [corresponding to exons 1–4, lacking the sequence from 368 aa to 458 aa (91 aa) and having an additional sequence, LDICCSP, in its C-terminus] and hPLEIAD-C (exons 5–12) were coexpressed with CAPN3:WT or CAPN3:CS in COS7 cells. PLEIAD homologs identified by psi-BLAST search share homology with the sequence of hPLEIAD-C (Tables 2 and 3). (b) When the C-terminal region, hPLEIAD-C, was coexpressed, the 94-kDa band of CAPN3:WT was visible (lane 3). However, the effect was not as dramatic as that observed with full-length PLEIAD (Fig. 1d, lanes 4 and 8). Notably, in the same sample, the intensity of the bands for autolyzed fragments was increased. The same patterns were observed for cells in which CAPN3:CS was coexpressed with either fragment of PLEIAD (lanes 6 and 7). Closed and open arrowheads indicate the full-length and autolytic fragments of CAPN3, respectively, detected by Western blotting using an anti-pIS2 antibody. (c) Mouse PLEIAD, mPLEIAD/LOC319719, is encoded by *Pleiad* (originally called *4732471D19Rik*). In this gene, the exons corresponding to exons 2 and 3 in the human *PLEIAD* are not defined. The largest gene product (mPLEIADa) is composed of 1354 aa, which is much larger than any isoforms of hPLEIAD. The structure of mPLEIADb is essentially identical with that of hPLEIADc. S3 and AS2 indicate the position of primers used in (d). The primer sequences are summarized in Table 1. (d) Expression of *Pleiad* detected by RT-PCR. In myotubes, a splicing variant of CAPN3 without exons 15 and 16 was also faintly detected (lane 11, lower band). W, H_2O was used as a template; – and +, isolated total RNA before and after, respectively, the RT reaction, was used as template; M, size marker. Qc, quadriceps from a 30-week-old mouse; Mt5, myotubes developed for 5 days from a primary culture of mouse myoblasts. Expected product sizes for *Capn3* (by primers CAPN3_411 and 412) and *Pleiad* (S3 and AS2) were 547 bp and 492 bp, respectively.

however, two markedly different features: the exons corresponding to human exons 2 and 3 are not identifiable, and exon 2, which by definition corresponds to human exon 4, is expanded (Fig. 2c). Reverse transcription (RT)-PCR analysis using primers S3 and AS2 (Fig. 2c) revealed that

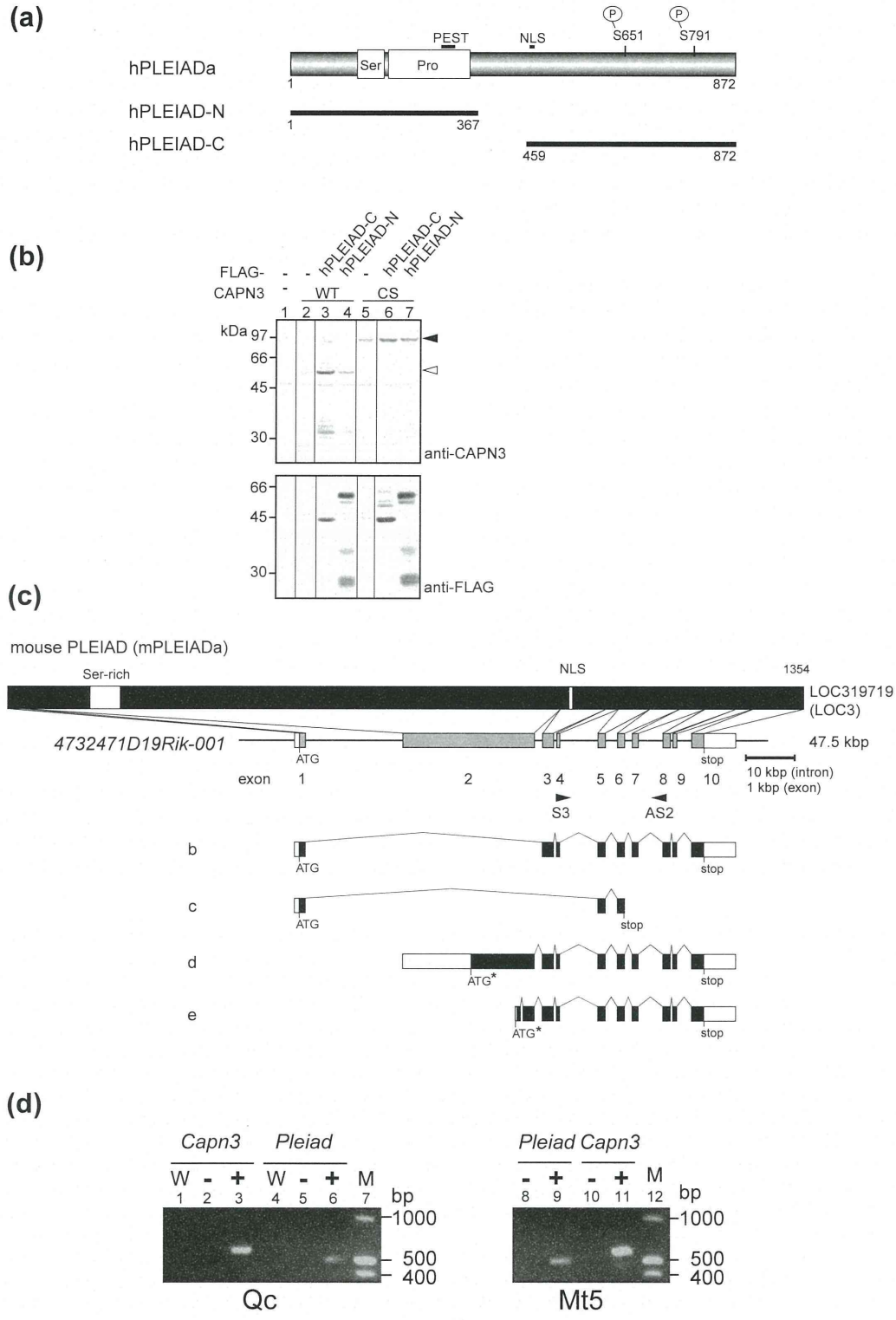

Fig. 2 (*legend on previous page*)

Table 1. Primers used in this study for cDNA cloning and RT-PCR detection

Primer	Reference sequence no.	Position[a]	Sequence
S1	BC037298	143–159s	cggtcggtaCCCGyAGCCATGGAGGA[b]
S2		417–439s	aacacatATGGCACCAGCATCTGCTTCTGG[b]
S3[c]		2071–2090s	TCACCTATGTCATGGAGGAA
AS1		3065–3048as	GGAGAGAGAGTTCAGGAGG
AS2[c]		2545–2562as	GGTGGCTTTCCATGGTAG
AS3		2155–2170as	AGGGTCTGCTGAAAGT
AS4		739–759as	GGTCCAAATCTACAGGATCAC
CAPN3_411	NM_000070.2	1801–1820s	CTCTT CACCA TTGGC TTCGC,
CAPN3_412		2347–2367as	CAGGTCCTTGTGTTTGTTCAC

[a] s, sense strand (5′ → 3′); as, antisense strand (5′ ← 3′).
[b] Lowercase letters indicate the sequence added or modified for cloning purposes.
[c] The sequences of these primers coincide with the corresponding mouse *Pleiad* sequences and, thus, were also used for amplification of mouse cDNA.

transcripts encoding the conserved C-terminal region of mPLEIADa are expressed in mouse skm cells (Fig. 2d, lanes 6 and 9).

A psi-BLAST homology search of databases using the human PLEIAD (hPLEIAD) sequence as a seed revealed significant conservation of the C-terminal half of hPLEIAD, corresponding approximately to exons 5–12 (hPLEIAD-C), among vertebrates (Fig. 2a and Tables 2 and 3). In contrast, the sequence of the N-terminal half of hPLEIAD, hPLEIAD-N, was not an efficient seed for retrieving a conserved structure among vertebrate PLEIAD homologs. These observations suggest that the regulation of CAPN3 autolysis was conducted by the C-terminal region of PLEIAD homologs during evolution.

PLEIAD interacts with CTBP1, a potential CAPN3 substrate

Yeast two-hybrid (YTH) screening identified CTBP1 as an interacting protein candidate for PLEIAD. CTBP1 is a highly conserved transcriptional co-repressor, and its structure–function relationships have been well studied (Fig. 3a).[34] In addition to hPLEIADa, which was originally used as a bait construct for the screening, hPLEIADf also interacted with CTBP1 (data not shown). In contrast to PLEIAD's effect on CAPN3's autolysis, PLEIAD's N-terminal region was sufficient for its interaction with CTBP1 (Fig. 3b, column D).

To characterize the mechanism of the CTBP1–PLEIAD interaction, we examined mutations that have been shown to abrogate CTBP1's interaction with the PLDLS motif in target proteins (Fig. 3b, columns F and H). Examining two mutants, A52E and V66R, did not demonstrate the interaction with hPLEIADa, hPLEIAD-N, or hPLEIADf:ex4term (2F to 4F and 2H to 4H). Therefore, it is possible that the structure of CTBP1 critical for its formation of co-repressor complexes is also involved in its interaction with PLEIAD. On the other hand, mutations in NAD(H)-binding domain of CTBP1 caused autoactivation of

Table 2. Amino acid sequences of PLEIAD homologs used in this study

Species (abbreviation)	General name	Accession no.[a]	Size (aa)	Homologous region[b] (aa)
Homo sapiens (*H. s.*)	Human	Q8NDZ2	872	459–872
Mus musculus (*M. m.*)	Mouse	NP_795961.3	1354	945–1354
Bos taurus (*B. t.*)	Bovine	XP_002690456.1	451	44–451
M. domestica (*M. d.*)	Opossum	XP_001380898.1	865	461–865
Gallus gallus (*G. g.*)	Chicken	XP_414554.1	646	245–646
Taeniopygia guttata (*T. g.*)	Zebra finch	XP_002194388.1	605	210–605
Meleagris gallopavo (*M. g.*)	Turkey	XP_003210405.1[c] (ENSMGAT00000005306)	433	32–433
Anolis carolinensis (*A. c.*)	Green anole lizard	XP_003227968.1[c] (ENSACAT00000006428)	441	47–441
Xenopus tropicalis (*X. t.*)	Western clawed frog	XP_002938112.1[c] (NW_003163664, ENSXETT00000064005, EL834443)	587	215–587
Oreochromis niloticus (*O. n.*)	Cichlid fish	XP_003455259.1[c] (NT_167549)	426	43–426
Tetraodon nigroviridis (*T. n.*)	Puffer fish	CAF92416[c,d] (CAAE01009900)	316	54–316
Danio rerio (*D. r.*)	Zebra fish	XP_001922583.1[c] (ENSDART00000129265)	770	381–770

[a] Data were retrieved from NCBI and Ensembl databases.
[b] Amino acid sequences corresponding to those encoded by exons 5–12 (459–872) in the human C5orf25 gene were used for analysis.
[c] The sequence was revised using genomic and EST sequences shown in parentheses.
[d] Gaps were left unfiled in consideration of uncertainty of deposited genome sequences.